1. Supplementary figures and tables

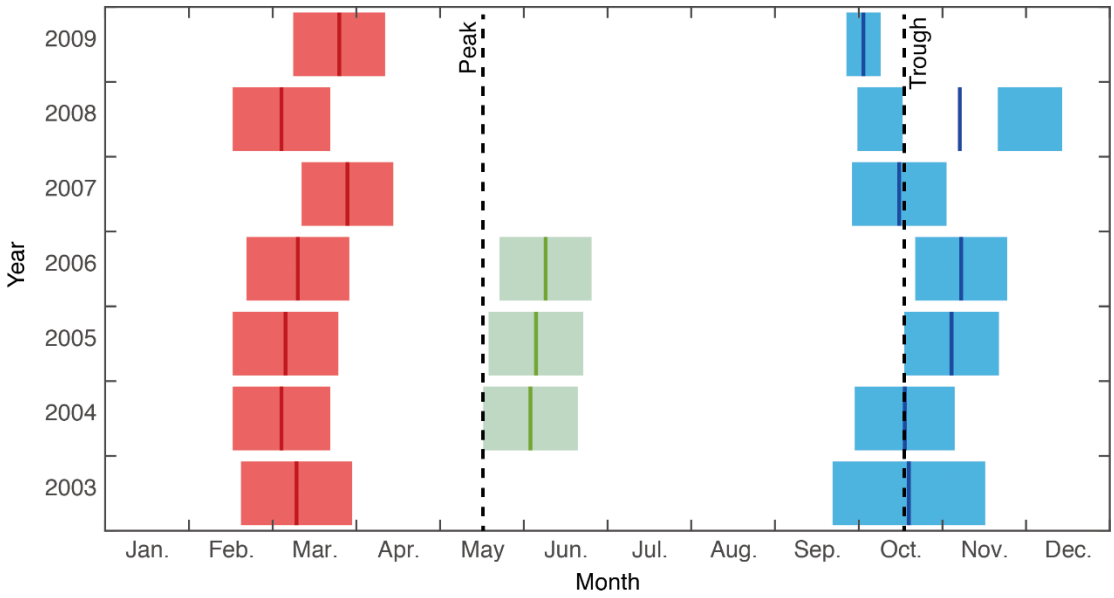

Figure S1. ICESat operational periods. The observations are categorized into three seasons. The middle of each period is taken as the observation time. The seasonal mass variations of glacier and snow in the SET based on GRACE have peak and trough values in May and in October, respectively.

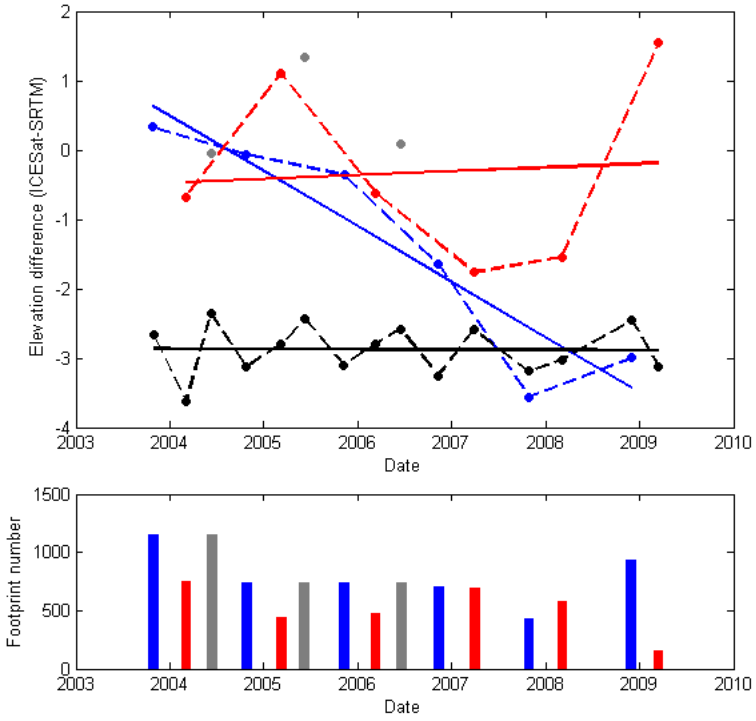

Figure S2. Surface height change of glaciers in the SET. (Top) Elevation difference of glaciers in October/November (blue), March (red) and June (gray). The black shows the result on a non-glacier region. (Bottom) The number of footprints. The result in 2009 has too few footprints and is not used.

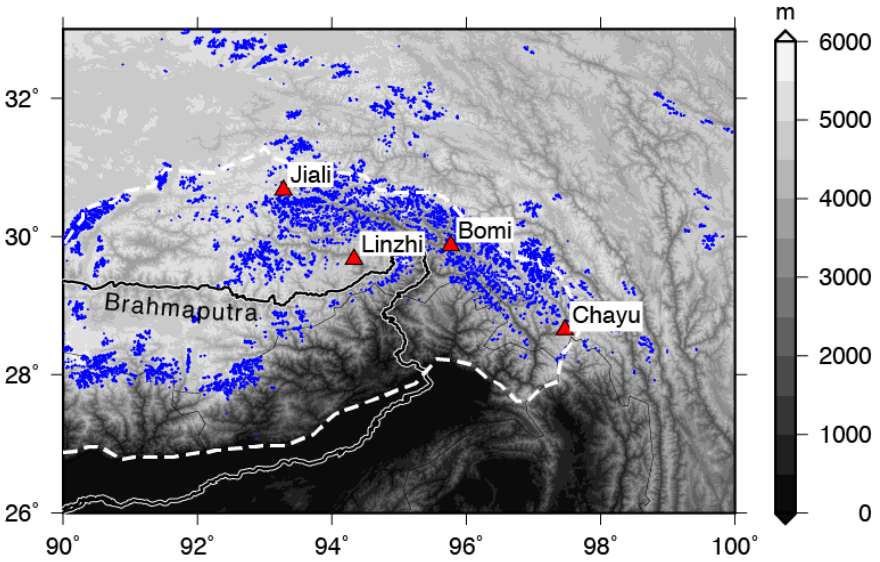

Figure S3. Locations of four meteorological stations in the study region. The gray background shows the topography, and the blue dots represent the distribution of glaciers. The boundary of the upper Brahmaputra Basin is marked by the dashed white curve.

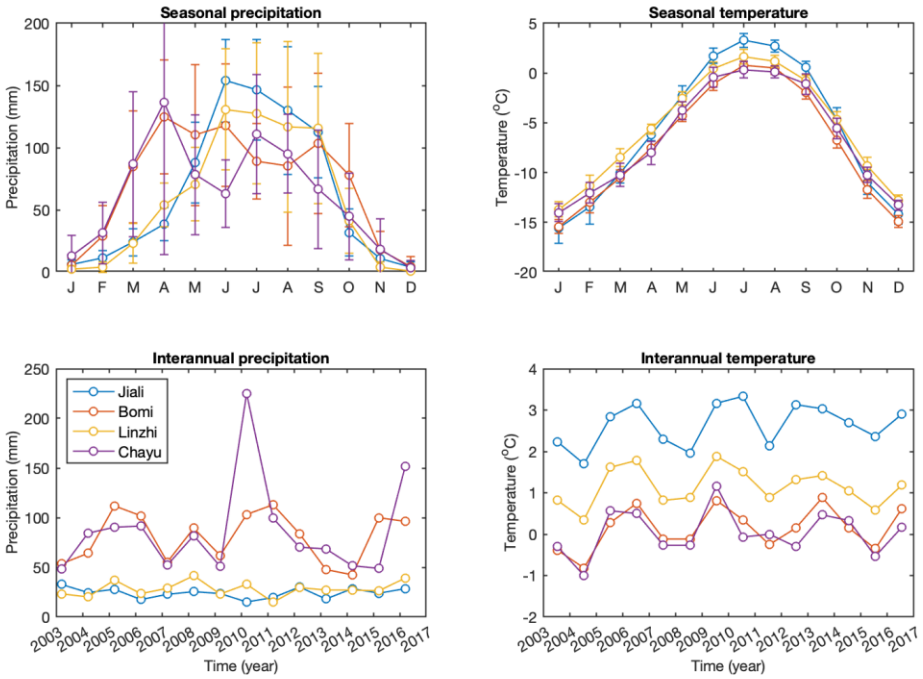

Figure S4. Seasonal and interannual changes in precipitation and temperature in the weather stations shown in Fig. S3. The error bars are calculated by the dispersions among the years.

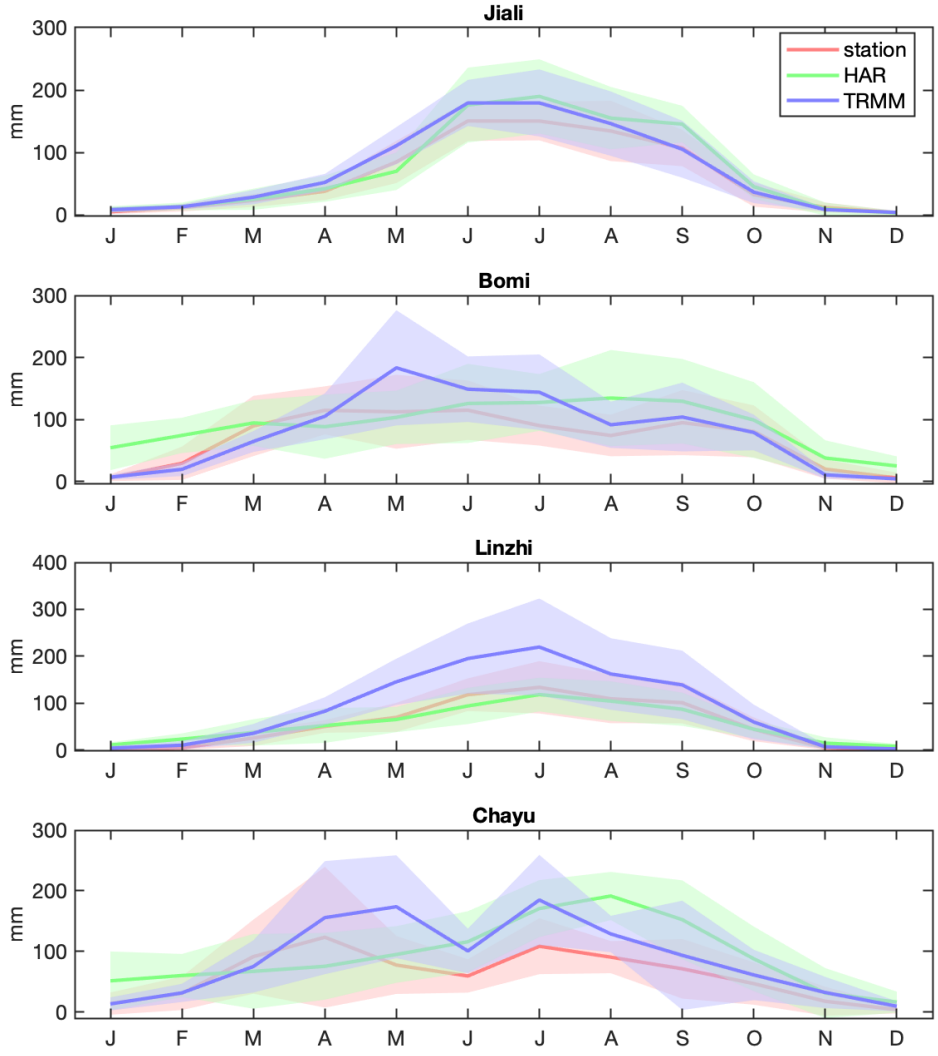

Figure S5. Comparison of seasonal precipitation results from meteorological stations, HAR and TRMM.

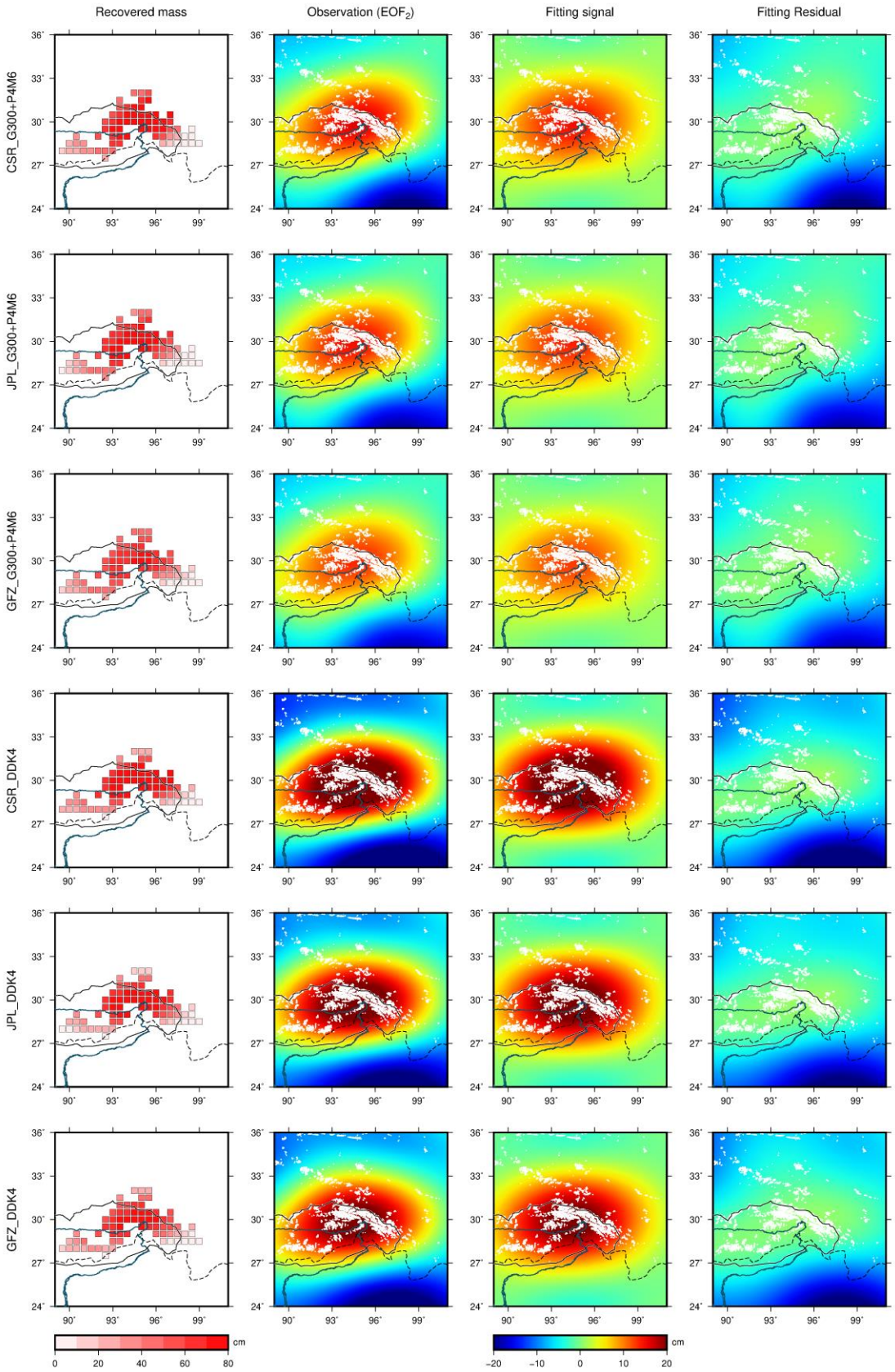

Figure S6. Recovered mass changes from the second EOF of different datasets and filters. The combination of each row is annotated to the left.

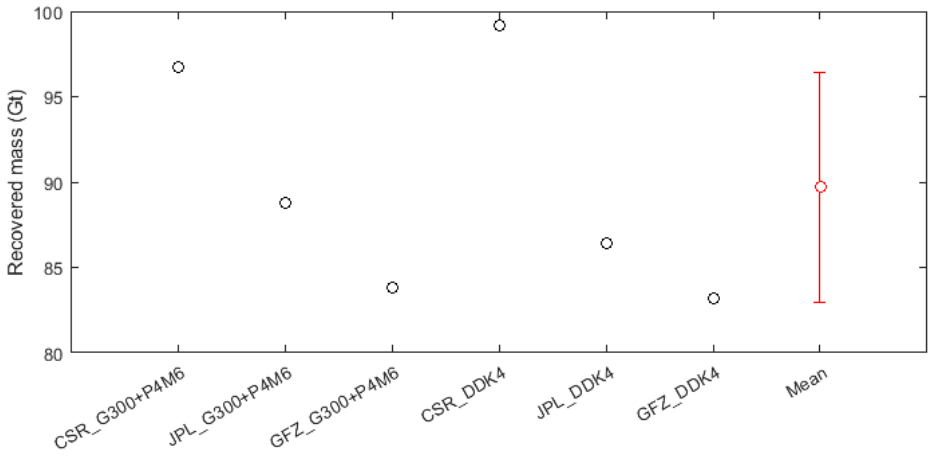

Figure S7. Recovered mass changes and their mean. The uncertainty is estimated based on the standard deviation.

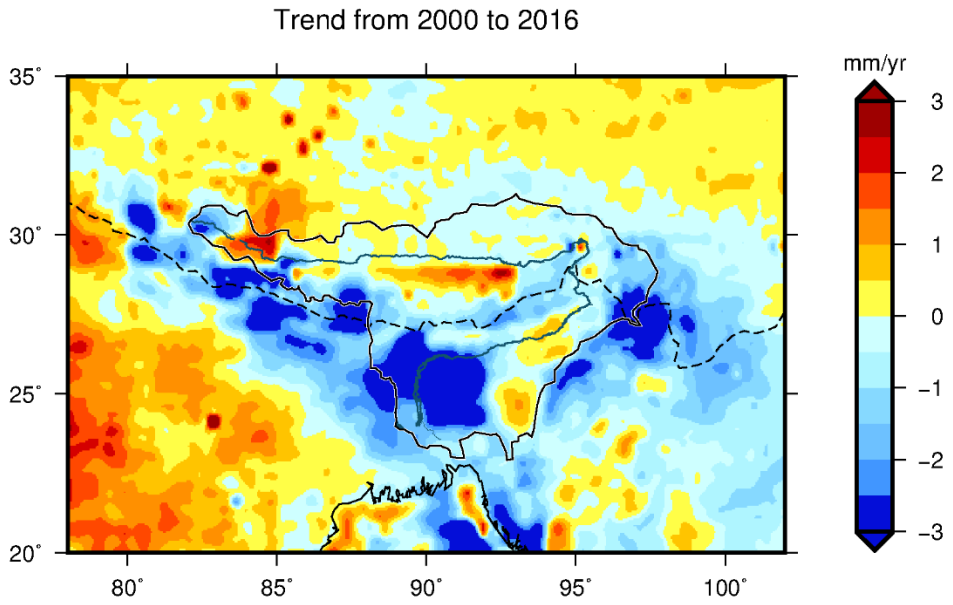

Figure S8. Trend of precipitation from 2000 to 2016 in the study region by using the TRMM product.

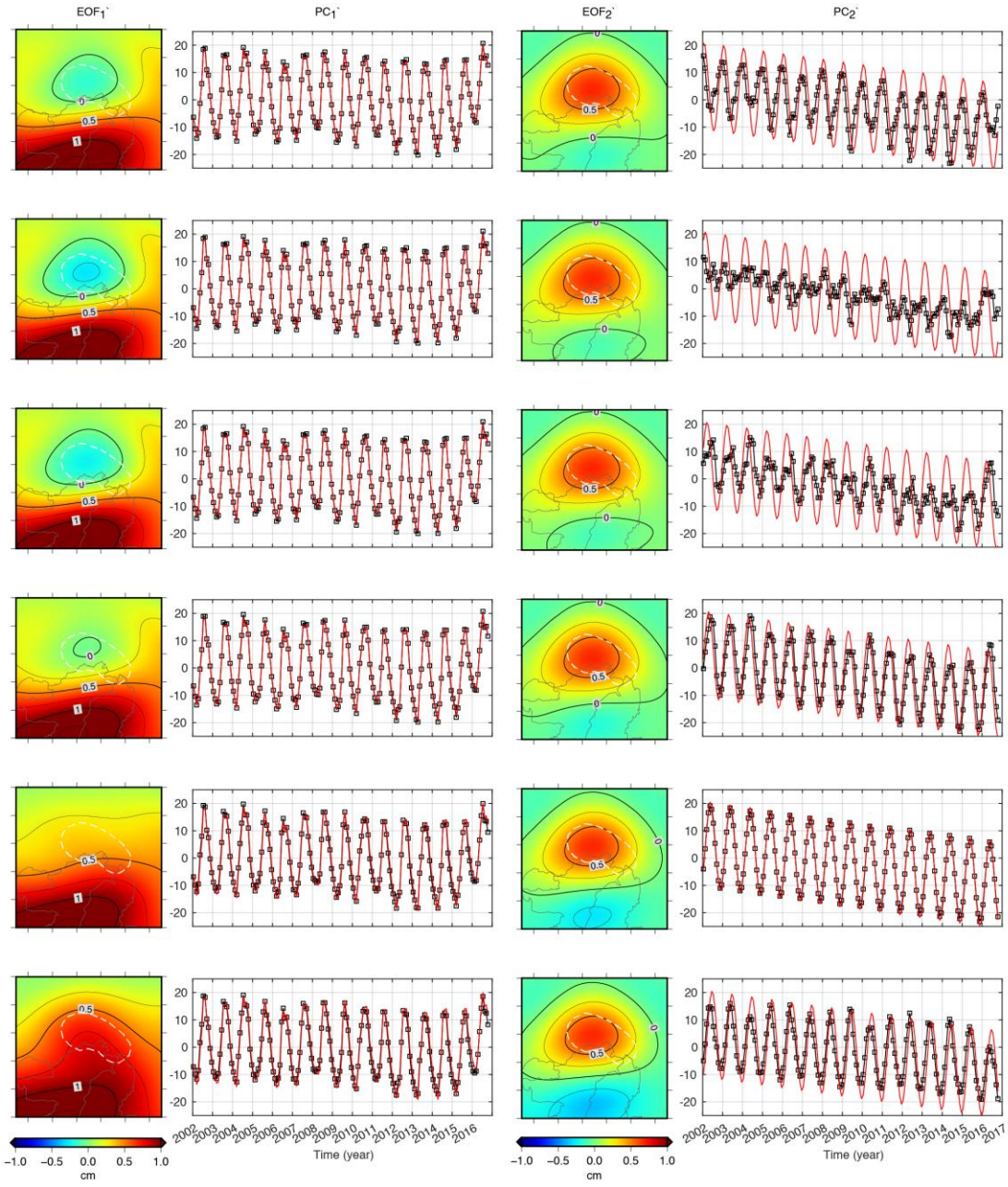

Figure S9. The first two modes of the EOF analysis of various mass simulations in the southeastern Tibet. The GS mass change has a peak month gradually shifting from January to June (from top to bottom). Refer to the text for the details about the models. The white dashed circle in each EOF plot roughly marks the glacierized area. The red curve in each PC plot shows the modeled series, and the black shows the PC.

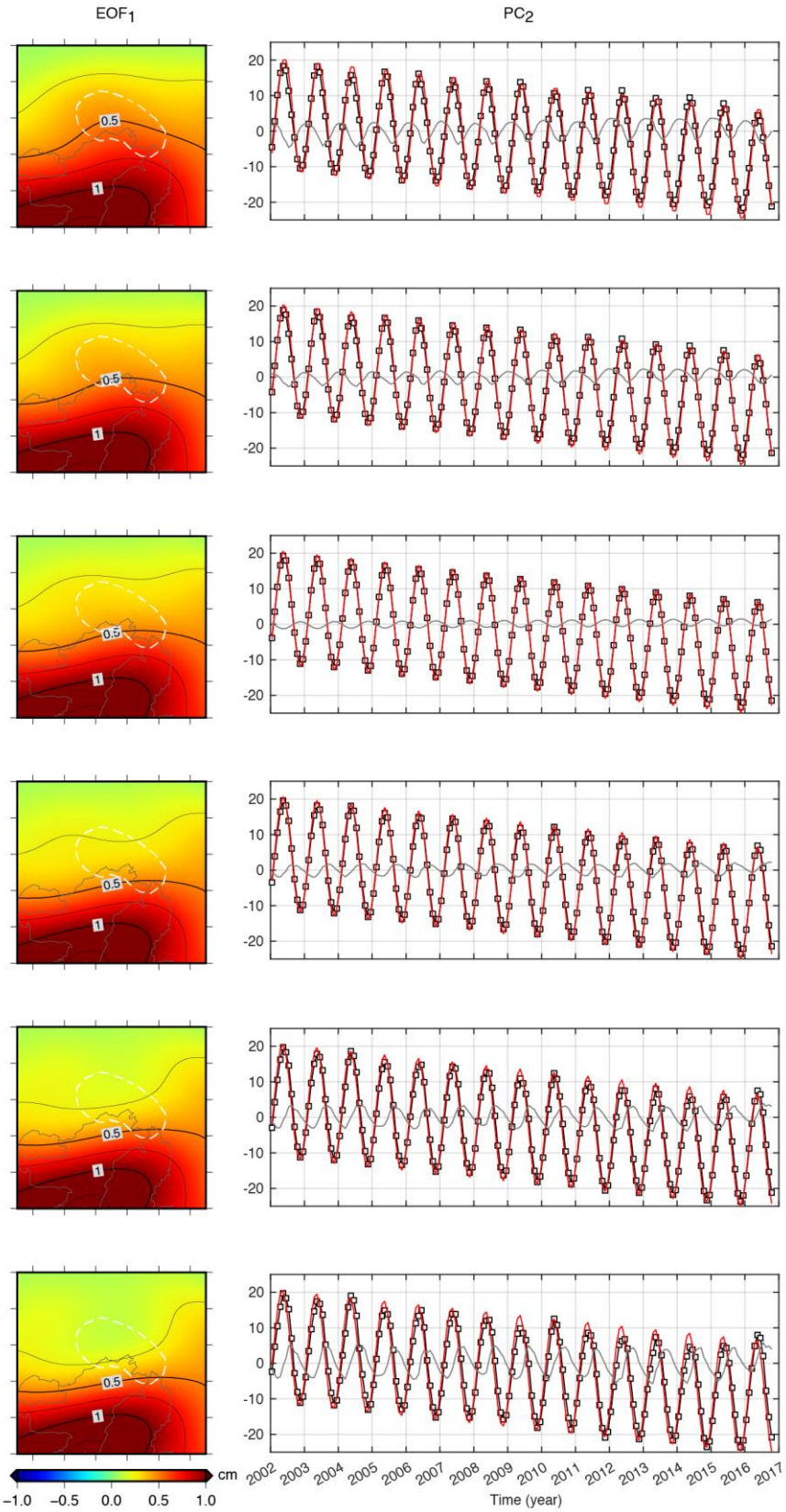

Figure S10. Same as Figure S10, but the peak date of glaciers is shifted from May 1st to May 26th by a 5-day interval (from top to bottom), and only EOF_1 and PC_2 are shown. The gray series in each PC plot show the difference of PC_2 relative to the modeled value.

Table S1. Geographic information of four meteorological stations.

Station	Longitude	Latitude	Elevation
Jiali	93.28	30.67	4488.8
Bomi	95.77	29.87	2736.0
Linzhi	94.33	29.67	2991.8
Chayu	97.47	28.65	2327.6

Table S2. GRACE error sources. (Unit: Gt/yr)

Source	Error	Remark
Linear Fit	0.14	Calculated from fitting residuals of a linear and trigonometric model
Data solution and smoothing errors	0.44	Estimated from the dispersion among CSR, GFZ and JPL with DDK4/G300+P4M6
Leakage error	0.51	The average peak date may vary from May 6th to May 16th
GIA	0.02	Difference between results with and without A's GIA model (A et al., 2013)
LIA	0.20	The total LIA effect in the whole Himalaya range and southeastern Tibet is -1±1 Gt/yr
Denudation	0.32	The total denudation effect in the eastern and southeastern Tibetan Plateau is 0.8 km^3/yr
Total	0.78	

2. Introduction of EOF

Generally, geophysical observations in the *i*th time epoch span a two-dimensional range, but they can be reorganized into a column vector $X_{:,i}$ (n grids). These column vectors during the whole study period (t epochs) can form a matrix X with size $n \times t$. In the

second step, singular value decomposition (SVD) method can be adopted to find orthogonal bases in the spatial and temporal domains:

$$X = USV'$$

where both U and V are orthonormal matrixes. S is a diagonal matrix and its diagonal elements are singular values of X. The matrix X is decomposed into N modes:

$$X = \sum_{i=1}^{N} U_{.,i} \times s_i \times V'_{.,i}$$

where $N = \min(n,t)$ and s_i is the ith diagonal element of S. The ith mode is composed of three items. Here, $U_{.,i} \times s_i$ is defined as the ith EOF (named EOFi) and $V_{.,i}$ is defined as the ith principle component (named PCi). EOFi can be rearranged back to the spatial distribution which the original observations ($X_{.,i}$) have. Then, EOFi and PCi represent the spatial feature and the temporal evolution of the ith mode, respectively. For a better readability, PCi is rescaled by a factor of a to make its maximum absolute value equals 1, and EOFi is rescaled correspondingly by a factor of $1/a$ so that the ith mode remains unchanged.

Since both variations of $U_{.,i}$ and $V_{.,i}$ are ones, s_i represents the explained variation of the ith mode:

$$\mathrm{EV}i = s_i^2 / \sum_{i=1}^{N} s_i^2$$

Because s is already in the descending order due to features of the SVD method, the EV is then also in the descending order, which means that the first modes explain the majority of the observations. Due to this characteristic, the EOF technique is often used to reduce the data amount and/or to improve the signal-noise-ratio by discarding the higher modes (Hannachi et al., 2007; Wouters and Schrama, 2007). In this study, the EOF method is used to separate gravity signals respectively caused by liquid and solid water, as they have different spatial domains (vast compared with local) and seasonal variations (an interval of three months in their peak months).

All EOFs/PCs are mathematically orthogonal to each other, and their geophysical explanation should be made with caution. Only limited modes can be explained by geophysical processes and one process may influence several modes (Eom et al., 2017). In this study region, terrestrial water storage change is the dominant source for seasonal

gravity change so it's likely to be reflected in the first mode. We compare EOF1 and PC1 of GRACE observations with these from soil moisture (GLDAS/NOAH) and precipitation (TRMM), and the good resemblance confirms that the first mode of GRACE observations is caused by terrestrial water storage change.

3. Further Discussion on the method and result

3.1. The orthogonality of the GS and water storage signals in GRACE observations

The orthogonality lies in the fact that the GS signal peaks exactly in May, which is not confirmed by other observations. We do find that the PC_2 of GRACE observations reaches a peak value in May, but it may be caused by our EOF analysis. Therefore, we conduct various GS mass modeling to test whether the orthogonality is artificial. Only water storage change and GS mass change are considered in the numeric modeling. The water storage change is obtained directly from the first mode of the decomposition of the GLDAS/NOAH model, and the GS mass change m is determined by an annual variation and a linear trend, as shown the equation below:

$$m_i = Acos\left(\frac{2\pi}{T} \times (t - \varphi_i)\right) + at \quad (4)$$

Where t is the observation time, A and φ are the amplitude and phase of the seasonal variation, and a is the trend. The peak month φ_i is gradually shifted from January to June (if the GS mass reaches the maximum between July and December then it contradicts the ICESat observation), so there are six models. Based on the relative magnitude between the first two modes in the EOF analysis of GRACE, the amplitude A and trend a are determined to be 16 cm w.e. and -1 cm w.e. yr^{-1}, respectively.

The result is shown in Figure S9. The first mode composed by EOF_1 and PC_1 represents water storage change and the second composed by EOF_2 and PC_2 represents GS mass change. The red curves in the PC plots represent the modeled series, and their consistency with the decomposed series (the black curves) demonstrates the effectivity

of our method. Two conclusions can be made. First, only in the case of May can we fully restore the GS mass change (i.e., a good agreement between the red and the black curves). Second, The PC_1 and EOF_2 are insensitive to the shift in month, while EOF_1 and PC_2 are sensitive. Besides, EOF_1 and PC_2 are always coupled so EOF_1 can be used to evaluate whether the PC_2 is well restored, or whether a leakage happens. If a leakage happens, an abnormal bulge can be identified in the glacierized zone (marked by the white dash circle) in EOF_1. This bulge shows how the compensation from the hydrological signal distorts its own spatial pattern. In fact, the bulge exists in all cases except May. If we look back at Figure 3 in the manuscript, we can find the EOF_1 of GRACE does not have such a bulge, which indicates that the GS signal can only peak in May and that the leakage from the hydrological signal is little, even if it exists.

Here, the orthogonality maintains if the GS peaks in November, but it is unrealistic for three reasons. First, it implies that the GS accumulates in summer and autumn, and melts in winter and spring, which is unlikely to happen in the northern hemisphere. Second, if it is realistic, it means that the PC_2 series should be multiplied by -1 (so it peaks in November), but it simultaneously inverts the long-term mass loss to mass increase, and GS mass increase contradicts current observations. Third, the ICESat observation clearly shows that glacier surface elevation is higher in the first half of the year.

3.2. Error estimation

The errors in the GRACE estimate include these components: data error, smoothing error, and leakage error. We have adopted three different solutions and two smoothing techniques to investigate the data error and smoothing error, the sum of which is 0.44 Gt/yr. The leakage error is determined by how effectively the hydrological and glacial signals are separated by the EOF technique. After the EOF decomposition, the negative trend in the glacierized area consists of 36% from mode 1 and 64% from mode 2, and the higher modes are negligible (about 0.2%). As shown above, it's assumed that the first mode is hydrological and the second is glacial. If a leakage happens, the negative

trend in the glacierized area in the first mode can be either underestimated (so the hydrological signal is leaked into the second mode to make the glacial signal overestimated) or overestimated (so the glacier signal is underestimated).

As we have shown above, the glacier mass change peaks in May. We can only determine the month without the exact day of the month due to the temporal resolution of GRACE. However, a time shift in weeks may slightly deteriorate the temporal orthogonality so a moderate leakage can still take place. We model glacier mass change in different days in May to investigate this possibility. The peak month is shifted from May 1st to May 26th by a 5-day interval and the result of EOF_1 and PC_2 is shown in Figure S10. In the glacierized zone, the bulge gradually decreases from May 1st and reaches a minimum in May 11th, and turned negative afterwards. By comparing with the EOF_1 of GRACE (Figure 3), we can identify that the peak date of the realistic glacier mass change is possibly to locate from May 6th to May 16th (the bulge is too evident in other cases), and this time range is used for leakage error estimation. Based on the residual between modeled and recovered glacier mass change, it is estimated that the residual may have a trend of up to 9% and a seasonal variation of up to 11% of the modeled glacier mass change. These values are used to estimate the leakage error.

There are potential errors from other signal sources, like glacial isostatic adjustment (GIA), little ice age (LIA) and weather denudation. The GIA effect which originates from polar regions has been corrected by A's GIA model (A et al., 2013), although its influence on the trend is as small as 0.02 Gt/yr. The main reason is that the spatial pattern of GIA is quite smooth, so it mainly influences the first mode and little leaks into the second one. This feature also holds for other signal sources: unless they exactly locate in the glacierized area, their influence will be reduced by the EOF decomposition. The effects of LIA and denudation are estimated to be -1 ± 1 Gt/yr (Jacob et al., 2012) and 1.6 Gt/yr (assuming the sediment has a density of 2 Gt/km^3) (Sun et al., 2009) in the vast south and southeastern Tibetan Plateau (over 500,000 km^2). Our glaciers and its peripheral region have an area of about 100,000 km^2, one fifth of the whole region, so we suppose their contribution to the glacier estimate is also proportionally 1/5. However, as we explain above, we could not precisely quantify their

contribution without knowing their spatial distribution, and they are more likely to be absorbed by the first mode, so we only include their contribution in the error estimation without correcting them in the trend. The sum of GRACE error estimation in the secular trend is summarized in Table S2.

4. Reference

A, G., Wahr, J., Zhong, S., 2013. Computations of the viscoelastic response of a 3-D compressible Earth to surface loading: an application to Glacial Isostatic Adjustment in Antarctica and Canada. Geophysical Journal International, 192(2): 557-572.

Eom, J., Seo, K.-W., Ryu, D., 2017. Estimation of Amazon River discharge based on EOF analysis of GRACE gravity data. Remote Sensing of Environment, 191: 55-66. DOI:10.1016/j.rse.2017.01.011

Hannachi, A., Jolliffe, I.T., Stephenson, D.B., 2007. Empirical orthogonal functions and related techniques in atmospheric science: A review. International Journal of Climatology, 27(9): 1119-1152. DOI:10.1002/joc.1499

Jacob, T., Wahr, J., Pfeffer, W.T., Swenson, S., 2012. Recent contributions of glaciers and ice caps to sea level rise. Nature, 482(7386): 514-518. DOI:10.1038/nature10847

Sun, W.K. et al., 2009. Gravity and GPS measurements reveal mass loss beneath the Tibetan Plateau: Geodetic evidence of increasing crustal thickness. Geophysical Research Letters, 36. DOI:10.1029/2008gl036512

Wouters, B., Schrama, E.J.O., 2007. Improved accuracy of GRACE gravity solutions through empirical orthogonal function filtering of spherical harmonics. Geophysical Research Letters, 34(23): n/a-n/a. DOI:10.1029/2007gl032098